

Optimizing AUV speed dynamics with a data-driven Koopman operator approach

Zhiliang Liu^{a,*}, Xin Zhao^b, Peng Cai^b, Bing Cong^a

^a*School of Automation, Qingdao University, Qingdao, 266071, China*

^b*PLA Naval Submarine Academy, Qingdao, 266199, China*

Abstract

Autonomous Underwater Vehicles (AUVs) play an essential role in modern ocean exploration, and their speed control systems are fundamental to their efficient operation. Like many other robotic systems, AUVs exhibit multi-variable nonlinear dynamics and face various constraints, including state limitations, input constraints, and constraints on the increment input, making controller design challenging and requiring significant effort and time. This paper addresses these challenges by employing a data-driven Koopman operator theory combined with Model Predictive Control (MPC), which takes into account the aforementioned constraints. The proposed approach not only ensures the performance of the AUV under state and input limitations but also considers the variation in incremental input to prevent rapid and potentially damaging changes to the vehicle's operation. Additionally, we develop a platform based on ROS2 and Gazebo to validate the effectiveness of the proposed algorithms, providing new control strategies for underwater ve-

*Corresponding author

Email addresses: liuzhiliang@qdu.edu.cn (Zhiliang Liu), 15886201166@163.com (Bing Cong)

hicles against the complex and dynamic nature of underwater environments.

Keywords:

Autonomous underwater vehicles, Data-driven, Koompman operator,
Model predictive control, Gazebo

1. Introduction

AUVs play an essential role in modern ocean exploration, which are capable of performing a variety of tasks, including but not limited to underwater surveying, detection, mapping of seafloor topography, collection of geological and hydrological data, as well as potential military applications. The development of AUV technology has significantly progressed over time, with modern AUVs featuring six degrees of freedom and capable of traveling at speeds exceeding 20 meters per second (Sahoo et al., 2019). These advancements have made AUVs more compact and less expensive, yet achieving full autonomy for these systems remains a significant challenge (Zhang et al., 2023; Gafurov and Klochkov, 2015).

AUVs have the capability to control their position and attitude in six degrees of freedom (DOFs). The 6-DOFs equation of motion for these vehicles often be partitioned into three relatively independent subsystems: speed control, longitudinal dynamics (encompassing parameters such as surge, heave, and pitch), and lateral dynamics (incorporating variables like sway, roll, and yaw) (Healey and Marco, 1992). This decomposition is particularly advantageous for slender symmetrical bodies, such as aircraft, missiles, and submarines (Gertler and Hagen, 1967).

This paper primarily focuses on the speed control system, which regulates

the speed of underwater vehicles by controlling the rotational speed of the propeller. The relationship between the propeller’s rotational speed and the vehicle’s speed is highly nonlinear, posing significant challenges in modeling and control. To resolve the difficulties, many thruster models have been proposed. Yoerger et al. (1990) provide valuable insights into the behavior and control of torque-controlled thrusters, offering potential strategies for improving their performance and reliability. Healey et al. (1995) formulate a two-state model that incorporates tinfoil propeller hydrodynamics, utilizing sinusoidal functions for lift and drag. Kim and Chung (2006) propose an accurate and practical thrust modeling for underwater vehicles that considers the effects of ambient flow velocity and angle. Bachmayer and Whitcomb (2003) utilize a least-squares regression method to interpret the experimental data, aiming to optimally adjust the model parameters for an accurate fit. Di Vito and Antonelli (2017) study the influence of ocean currents on the closed-loop performance of thrusters, considering both the dynamics of the thrusters and the impact of ocean currents.

Existing methods often simplify this nonlinear system into a linear one, which may not fully capture the system’s complexities. Moreover, obtaining an accurate model of the system can be challenging in practical engineering applications, adding complexity to the implementation of nonlinear control methods(Gong et al., 2021; Shen et al., 2017; Yan et al., 2023). Additionally, some approaches without a specific model have not completely considering critical system constraints, such as the propeller’s speed limit and the increment input limit(Lin et al., 2023; Yan et al., 2019).

The Koopman operator theory offers a compelling approach to addressing

the non-linearity inherent in the speed control of AUVs. Unlike traditional linearization techniques, the Koopman method provides a linear representation of nonlinear dynamical systems by lifting the original state space into a higher-dimensional space where linear analysis can be applied (Mezić, 2005; Kutz et al., 2016). Dynamic Mode Decomposition (DMD) is a data-driven method for analyzing dynamical systems. The original DMD method primarily addresses linear systems (Rowley et al., 2009; Schmid, 2010). To analyze nonlinear systems, extensions such as Extended DMD (EDMD) and Higher-order DMD have been developed. Williams et al. (2015) provide a data-driven approximation of the Koopman operator, extending DMD’s capabilities to capture nonlinear dynamics. This results in a more accurate and comprehensive model of the system dynamics, which is particularly beneficial for capturing the complex behaviors of AUVs.

Model Predictive Control (MPC) complements the Koopman method by providing a robust framework for handling constraints and optimizing control inputs over a finite horizon (Korda and Mezić, 2018; Zhang et al., 2022b; Bruder et al., 2020). MPC’s ability to anticipate future events and adjust control actions accordingly makes it well-suited for managing the constraints of AUV speed control systems. By integrating the Koopman operator with MPC, we can leverage the strengths of both methods: the Koopman method’s enhanced modeling accuracy and MPC’s predictive and constraint-handling capabilities.

This study’s key contributions are as follows:

- This paper introduces a speed control system developed by integrating Koopman operator and MPC methods, designed to enhance the accuracy

and robustness of AUV speed control;

- The proposed control system takes into account the practical constraints on system input, states, and increment input, which allows for precise tracking of the AUV's trajectory;
- A simulation platform that integrates Gazebo and ROS2 has been designed to verify the effectiveness of the proposed solution, enabling comprehensive testing in a controlled environment and reducing the risk of mission failure prior to real-world application.

The structure of this paper is outlined as follows. Section 2 presents the velocity model for AUV. Section 3 introduces the theory of the Koopman operator and details the process for achieving a high-dimensional linear space. Section 4 discusses the integration of Koopman operator theory with MPC for its application in AUV. Section 5 presents two simulation experiments, one conducted in MATLAB and the other in the physical simulation software Gazebo. The final section is dedicated to a discussion of the conclusions drawn from the research.

Notation: \mathbb{C} , \mathbb{R} and \mathbb{Z} denote complex number, real number and integers, respectively. A^T , $\|A\|_F$ and $\|A\|_2$ denote transpose, Frobenius norm and Euclidean norm, respectively. Given matrices $A \in \mathbb{C}^{m \times n}$ and $B \in \mathbb{C}^{m \times d}$, we denote by $[A, B] \in \mathbb{C}^{m \times (n+d)}$ the matrix created by concatenating A and B . $\mathcal{T}u$ denotes next input, \mathcal{H} denotes Hilbert space. \min and \max denote the minimum and maximum value, respectively.

2. Problem formulation and preliminaries

In general, the force and moment vector of the thrust will be a complex function(Fossen, 2011). This relationship can be expressed as:

$$\tau = f(v, u), \quad (1)$$

where $v \in \mathbb{R}^6$ is the underwater vehicle's velocity vector, $u \in \mathbb{R}^p (p \geq 6)$ is the control variable, and f is a nonlinear vector function. The thrust T of a single-screw propeller can be obtained by the following formula:

$$T = \rho D^4 K_T (J_0) |s| s, \quad (2)$$

where s represents the propeller RPM(revolutions per minute), D represents the propeller diameter, ρ represents the water density, and V_a represents the propeller advance velocity (the velocity of the water flow entering the propeller). $J_0 = V_a / (sD)$ is an advanced number and K_T is the thrust coefficient. In general, the thrust in the forward and backward directions is not symmetrical. However, many underwater vehicle thruster systems are designed to provide symmetrical thrust. This parameter K_T typically exhibits linear behavior in J_0 , so the following approximation holds:

$$K_T = \alpha_1 + \alpha_2 \frac{V_a}{sD}. \quad (3)$$

In this case, α_1 and α_2 are two constants. And then, the thrust can be described as

$$T(s, V_a) = T_{|s|s} |s| s + T_{|s|V_a} |s| V_a, \quad (4)$$

where $T_{|s|s} > 0$ and $T_{|s|V_a} < 0$ are design parameters that depend on factors such as propeller diameter, duct shape, and water density. The above coeffi-

cients also depend on s and V_a , since the above two equations are only first-order approximations to more general expressions. However, experiments have shown that this dependence is negligible under most practical operating conditions. Forward speed relation to vehicle speed can be expressed as

$$V_a = (1 - \omega)V, \quad (5)$$

where ω is the wake fraction (typically $0.1 - 0.4$). The propeller force generated by a single propeller can be described by a nonlinear function according to the results of (4)

$$\tau = b_1|s|s - b_2|s|v, \quad (6)$$

where $b_1 = T_{|s|s} > 0, b_2 = -T_{|s|V_a}(1 - \omega)$.

Remark 1: In the multivariate case, Equation (4) can be rewritten as: $\tau = B_1u - B_2(u)v$, where B_1 and B_2 are matrices with appropriate dimensions, and v is a newly defined control variable, expressed as $u_i = s_i|s_i|$. As referenced in Fossen (2011), bilinear models are often approximated by simpler affine models (i.e., $\tau = Bu$) due to the limited theoretical framework for non-affine control systems. To address this, this study proposes applying Koopman theory and MPC method for direct control of non-affine systems.

2.1. Velocity control model

According to Healey and Marco (1992), the 6-DOFs equations of motion for an underwater vehicle can be divided into three non-interacting subsystems for speed control, steering, and diving. This paper focus on the speed control. Assuming negligible coupling between sway, heave, roll, pitch, and

yaw motions, the speed equation can be expressed as:

$$(m - X_{\dot{v}})\dot{v} = X_{|v|v}|v|v + (1 - t)T + x_e, \quad (7)$$

where m is the vehicle mass, u is the vehicle velocity, $X_{|v|v}$ is hydrodynamic parameter, T is thrust, x_e is external disturbance, $X_{\dot{v}}$ is the added inertia, t is the thruster deduction number. Combined equation (7) and (4)(ignoring the external disturbance x_e), one has

$$(m - X_{\dot{v}})\dot{v} = X_{|v|v}|v|v + (1 - t)(T_{|s|s}|s|s + T_{|s|V_a}|s|V_a) \quad (8)$$

The model under study is nonlinear, differing from the dynamics described in Fossen (2011). Consequently, traditional linear control methods are not applicable. In this study, we employ Koopman theory to derive a linear model in a higher-dimensional space. Subsequently, we use the MPC approach to design the control strategy. Equation (8) represents a continuous dynamical system. In practical applications, it is often necessary to utilize a discrete form of the system. Various discretization methods can be employed for this purpose, including the forward Euler method and Runge-Kutta methods.

3. Koopman Operator Theory

Consider the following discrete-time nonlinear system:

$$x_{k+1} = f(x_k), \quad (9)$$

where x_k is a state vector in the manifold $\mathcal{M} \subset \mathbb{R}^n$ on which x_k evolves. Here, $k \in \mathbb{Z}$ denotes discrete time, and $f : \mathcal{M} \rightarrow \mathcal{M}$ is the evolution operator.

To facilitate the analysis of this nonlinear system, we introduce the Koopman operator \mathcal{K} . According to Koopman (1931), the evolution of the system described by (9) can be recast in an infinite-dimensional function space as follows:

$$(\mathcal{K}\zeta)(x_k) = (\zeta \circ f)(x_k) = \zeta(x_{k+1}), \quad (10)$$

the Koopman operator \mathcal{K} thus defines a new dynamical system $(\mathcal{H}, n, \mathcal{K})$. In this context, $\zeta = [\zeta_1, \zeta_2, \dots, \zeta_\infty] \in \mathcal{H}$ represents a set of lifting functions, where each $\zeta_i : \mathbb{R}^n \rightarrow \mathbb{C}$ is termed an observable. Any scalar function of the state x_k can qualify as a lifting function. The symbol \circ denotes the composition of the lifting function ζ with the evolution function f .

The set of all such lifting functions forms an infinite-dimensional Hilbert space \mathcal{H} . The Koopman operator $\mathcal{K} : \mathcal{H} \rightarrow \mathcal{H}$ is a linear operator that acts on these scalar-valued lifting functions ζ within \mathcal{H} . It is important to note that the Koopman operator maps functions of the state space to other functions of the state space (i.e., $\mathcal{K} : \mathcal{H} \rightarrow \mathcal{H}$), rather than mapping states to states as $f : \mathcal{M} \rightarrow \mathcal{M}$ (Budišić et al., 2012).

Despite the fact that the Koopman operator \mathcal{K} acts on lifting functions ζ , making it potentially infinite-dimensional even when the original system f is finite-dimensional, it is often possible to approximate \mathcal{K} with a finite-dimensional matrix while retaining a high degree of accuracy. This approximation is crucial for practical applications, as the exact finite-dimensional representation of \mathcal{K} is generally infeasible.

According to Williams et al. (2015), the infinite-dimensional representation (10) is approximated as follows in finite dimensions:

$$\zeta(x_{k+1}) = \tilde{\mathcal{K}}\zeta(x_k) + r_k, \quad (11)$$

where $\zeta \in \mathbb{R}^N$, $N \gg n$. The matrix $\tilde{\mathcal{K}} \in \mathbb{R}^{N \times N}$ represents a finite-dimensional approximation of the Koopman operator \mathcal{K} , and $r_k \in \mathcal{H}$ is the residual term, capturing the approximation error.

This formulation enables the use of linear techniques to analyze and control the original nonlinear system, providing a powerful framework for understanding complex dynamical behaviors.

3.1. Dynamical System with Input

Consider the dynamical discrete nonlinear system with input:

$$x_{k+1} = f(x_k, u_k), \quad (12)$$

where $x_k \in \mathcal{M} \subseteq \mathbb{R}^n$ represents the state vector, and $u_k \in \mathcal{N} \subseteq \mathbb{R}^p$ represents the input vector. The evolution of the state is governed by the nonlinear function $f : \mathcal{M} \times \mathcal{N} \rightarrow \mathcal{M}$. To analyze and control this nonlinear system, we introduce the Koopman operator \mathcal{K} . Specifically, the Koopman operator \mathcal{K} acts on observable functions ζ defined on the state space. According to Koopman (1931), the Koopman operator for the system in (12) is defined as:

$$(\mathcal{K}\zeta)(x_k, u_k) = (\zeta \circ f)(x_k, u_k), \quad (13)$$

where $\zeta(x_k, u_k) = [\zeta_1(x_k, u_k), \zeta_2(x_k, u_k), \dots, \zeta_{N+p}(x_k, u_k)]$ is a vector of lifting functions, and each $\zeta_i : \mathbb{R}^n \times \mathbb{R}^p \rightarrow \mathbb{R}$ belongs to a space of observables \mathcal{H} .

The main objective of this work is to construct a finite-dimensional approximation of the Koopman operator, denoted as $\tilde{\mathcal{K}}$, and then use this approximation to predict the future states of the system. To achieve this, we define an extended state vector as follows:

$$\xi_k = \begin{bmatrix} x_k \\ u_k \end{bmatrix}, \quad (14)$$

the evolution of ξ_k can be described by:

$$\xi_{k+1} = F(\xi_k) = \begin{bmatrix} f(x_k, u_k) \\ \mathcal{T}u_k \end{bmatrix}, \quad (15)$$

where $\mathcal{T}u_k \in \mathbb{R}^p$. Consequently, equation (13) can be rewritten as:

$$(\mathcal{K}\zeta)(\xi) = (\zeta \circ f)(\xi). \quad (16)$$

To obtain the finite-dimensional approximation $\tilde{\mathcal{K}}$, we employ the EDMD algorithm (Williams et al., 2015). This algorithm uses a collection of data (ξ_{k+1}, ξ_k) that satisfies $\xi_{k+1} = F(\xi_k)$ to find the optimal approximation $\tilde{\mathcal{K}}$ by solving:

$$\min_{\tilde{\mathcal{K}}} \sum_{j=1}^N \|\zeta(\xi_{k+1}) - \tilde{\mathcal{K}}\zeta(\xi_k)\|_2^2. \quad (17)$$

By applying the Koopman theory, we can express the nonlinear system (12) in the following linear form:

$$\begin{aligned} z_{k+1} &= Az_k + Bu_k, \\ \hat{x}_k &= Cz_k, \end{aligned} \quad (18)$$

where $z_k = \phi(x_k) = [\phi_1(x_k), \phi_2(x_k), \dots, \phi_N(x_k)]^T \in \mathbb{R}^N$, and \hat{x}_k is the prediction of x_k . The matrices $A \in \mathbb{R}^{N \times N}$, $B \in \mathbb{R}^{N \times p}$, and $C \in \mathbb{R}^{n \times N}$ need to be identified. We assume that the vector of lifting functions can be expressed as $\zeta(\xi_k) = \phi(x_k) + u_k$, leading to:

$$\zeta_i(\xi) = \begin{bmatrix} z_k \\ u_k \end{bmatrix}. \quad (19)$$

The equation (17) can be reformulated as:

$$\min_{A,B} \sum_{j=1}^K \|\phi(x_{k+1}) - A\phi(x_k) - Bu_k\|_2^2. \quad (20)$$

The optimal matrix C can be computed as:

$$\min_C \sum_{j=1}^K \|x_j - C\phi(x_j)\|_2^2. \quad (21)$$

For simplicity, let $\phi_i = x_i$ for $i = 1, 2, \dots, n$, making $C = [I, 0]$, where I is an $n \times n$ identity matrix.

This theoretical framework allows for the application of linear control techniques to nonlinear systems, providing a powerful tool for analyzing and controlling complex dynamical systems. The use of EDMD to approximate the Koopman operator enables the practical implementation of this approach in real-world scenarios.

3.2. Finding the estimated Koopman operator

Assuming the following set of data

$$\begin{aligned} X &= \begin{bmatrix} x_1 & x_2 & \dots & x_L \end{bmatrix}, \\ Y &= \begin{bmatrix} y_1 & y_2 & \dots & y_L \end{bmatrix}, \\ U &= \begin{bmatrix} u_1 & u_2 & \dots & u_L \end{bmatrix}, \end{aligned} \quad (22)$$

where $y_k = f(x_k, u_k)$, this method does not impose the requirement for variables x_i and x_{i+1} to adhere to equal time intervals, nor does it necessitate that they originate from the same dynamic trajectory. This flexibility allows for the application of a broader dataset in analysis, free from the constraints of strict continuity typically associated with traditional time-series data.

After preparing the data, it is essential to apply the lifting function to map the data (X, Y) into the lifted space (\bar{X}, \bar{Y}) . There is no need to increase the dimensionality of U since predicting U is not required. The optimization problem is

$$\min_{A, B} \|\bar{Y} - A\bar{X} - BU\|_F, \quad (23)$$

where $\bar{Y} = [\phi(y_1), \phi(y_2), \dots, \phi(y_L)]$, $\bar{X} = [\phi(x_1), \phi(x_2), \dots, \phi(x_L)]$, $U = [u_1, u_2, \dots, u_L]$.

Tikhonov regularization, which adds a penalty based on the Frobenius norm of the matrix in question within a linear regression framework, can be employed to enhance the condition (23). This involves adjusting the EDMD cost function by incorporating a regularization term.

$$\begin{aligned} J(U; \alpha) &= \frac{1}{L} \|\bar{Y} - A\bar{X} - BU\|_F + \frac{\alpha}{L} \|[A, B]\|_F^2 \\ &= \frac{1}{L} \text{trace}((\bar{Y} - A\bar{X} - BU)(\bar{Y} - A\bar{X} - BU)^T) \\ &\quad + \frac{\alpha}{L} \text{trace}([A, B][A, B]^T) \end{aligned} \quad (24)$$

4. Koopman operator theory based MPC control

Unlike nonlinear MPC, which involves solving challenging nonconvex optimization problems and relies heavily on local solutions, the data-driven approach reduces computational demands. In this section, we detail the design of MPC controllers for nonlinear systems using Koopman operator theory.

4.1. MPC formulation

To simultaneously consider the constraints on both the input (rotational speed) and the increment input (rate of change of rotational speed), the

derived high-dimensional linear system $z_{k+1} = Az_k + Bu_k$ is transformed as follows:

$$\begin{bmatrix} z_{k+1} \\ u_k \end{bmatrix} = \begin{bmatrix} A & B \\ 0 & B \end{bmatrix} \begin{bmatrix} z_k \\ u_{k-1} \end{bmatrix} + \begin{bmatrix} 0 \\ B \end{bmatrix} \Delta u_{k-1}, \quad (25)$$

here, let $\bar{z}_k = [z_k, u_{k-1}]^T$, $\bar{A} = [A, B; 0, B]$, $\bar{B} = [0, B]^T$. Then the MPC formulation is described as follows:

$$\begin{aligned} \min_{\Delta u_k} \quad & J = \sum_{k=0}^{Nh-1} ((\hat{x}_k - y_r)^T Q_u (\hat{x}_k - y_r)) + \Delta u_k^T R \Delta u_k \\ & + ((\hat{x}_{Nh} - y_r)^T Q_N (\hat{x}_{Nh} - y_r)) \\ \text{s.t.} \quad & \begin{cases} \bar{z}_{k+1} = \bar{A} \bar{z}_k + \bar{B} \Delta u_k, \\ \hat{x}_k = C \bar{z}_k, \quad \hat{x}_{\min} \leq \hat{x}_k \leq \hat{x}_{\max}, \\ u_{\min} \leq u_k \leq u_{\max}, \quad \Delta u_{\min} \leq \Delta u_k \leq \Delta u_{\max}, \end{cases} \end{aligned} \quad (26)$$

where Q_u , R , Q_N are the weight matrices, Nh is the prediction horizon, \bar{z}_k is the modified lifting vector, \hat{x}_{\min} and \hat{x}_{\max} are constraints on the output vector, u_{\min} and u_{\max} are the constraints of RPM, Δu_{\min} and Δu_{\max} are the constraints of increment input.

Remark 2: Different from the work in Korda and Mezić (2018), this study considers the constraints on both the input and increment input. According to Korda and Mezić (2018), the number of constraints remains unaffected by the dimensionality of the lifting function. So, once we've figured out the nonlinear mapping $z_0 = \phi(x_k)$, solving (26) doesn't cost much more than solving a standard linear MPC problem for the same prediction horizon. This remains true even if both setups have the same number of control inputs and the state-space dimension is n rather than N .

5. Simulations and results

5.1. Simulation in MATLAB

The proposed approach is implemented to govern the dynamical system as outlined in equation (7). The system parameters are specified as follows: $m = 146.471kg$, $X_{\dot{v}} = -4.876161$, $X_{|v|v} = -6.2282$, $t = 0.1$, $\rho = 1000kg/m^3$, $D = 0.2m$, $\alpha_1 = 0.2$, $\alpha_2 = 0.1$, and $\omega = 0.1$.

An MPC controller is designed by utilizing exclusively input-output data, without knowing the model knowledge. The lifting-based predictor, as described by equation (18), is derived by discretizing the scaled dynamics with the Runge-Kutta fourth-order method over a sampling period of $T_s = 0.01$ seconds. A simulation of 1000 trajectories is conducted, with each trajectory encompassing 100 sampling periods, equivalent to 1 second. The control input for each trajectory is a uniformly distributed random signal within the range of $[-50, 50]$.

The initial conditions for these trajectories are randomly selected from a uniform distribution over the interval $v \in [-0.5, 0.5]$. This data collection yields matrices X and Y of dimensions 1×10^5 and a matrix U of size 1×10^5 . Notably, X and Y are composed of the underwater vehicle's velocity u , while U consists of the propeller's speed s . The lifting functions ϕ are chosen to represent the state itself, that is, $\phi_1 = v$. The centers of the gauss functions¹ are randomly selected from a uniform distribution over the interval $[-1, 1]$. Consequently, the dimension of the lifted state-space is set to $N = 5$.

Fig. 1 illustrates the comparison between the actual system states and

¹The gauss function with center at x_0 is defined by $\phi(x) = e^{-\frac{\|x-x_0\|^2}{2}}$.

the states predicted by the Koopman operator, starting from two randomly selected initial conditions within the range $v \in [-0.5, 0.5]$ ($v_0^1 = 0, v_0^2 = 0.1$). The control signal $s(t)$ is depicted as a periodic wave with a period of 0.1 second and the magnitude is 40. Fig. 1 shows that the lifting-based Koopman predictor predicts the true velocity well.

By applying the Tikhonov algorithm (24) with collection data X, Y and U , we can obtain the linear matrix expression (18). Following this, MPC algorithm is utilized to control the underwater vehicle's speed by adjusting the propeller speeds. Here, set $C = [1, 0, \dots, 0]$, select the cost function matrices as $Q_N = Q_u = 2000$ and $R = 0.01$. The prediction horizon is set to $Nh = 10$. In the simulation, the input s is imposed the constraint as $[-50, 50]$, the increment input is restricted as $[-20, 20]$, and a piece-wise reference $y_r(t)$ is tracked.

In Fig. 2, it is shown that even the maximum speed and the increment speed of the propeller are constrained, the vehicle can track a given reference speed with the proposed Koopman MPC algorithm. Fig. 3 illustrates that both the input and increment input are constrained, in which the maximum speed of the propeller is 50 (PRM), and the increment speed is 20.

Remark 3: The system under study in this paper cannot be linearized locally due to its inherent complexity. This scenario highlights the superiority of data-driven algorithms, which can effectively handle such complexities. The MPC algorithm is particularly advantageous as it can manage constraint issues. By integrating Koopman operator theory with MPC, the control of unknown nonlinear systems can be effectively addressed, while also managing constraints. This combination leverages the strengths of both theoretical

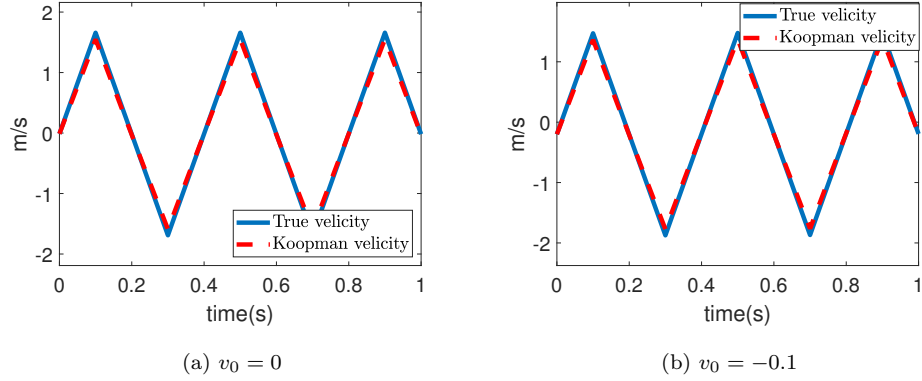


Figure 1: Prediction comparison for different initial value

frameworks to achieve control solutions.

5.2. Simulation in Gazebo

5.2.1. Simulation platform

In this study, we validate the proposed algorithm using open-source software, Gazebo and ROS. The operating system is Ubuntu 22.04(Intel(R) Core(TM) i7-7820HQ CPU @ 2.90GHz, 16G RAM), with Gazebo version Harmonic² and ROS version Iron³. The communication between Gazebo and ROS is facilitated by the ROS-Gazebo bridge⁴. The underwater vehicle model used for simulation is based on the model proposed in Player et al. (2023), with all parameters configurable through the plugin files. LRAUV Sim1 is based on the new Gazebo, which has been entirely rewritten and is fundamentally different from the classic version of Gazebo. This updated

²<https://gazebosim.org/docs/harmonic/getstarted/>

³<https://docs.ros.org/en/iron/Installation.html>

⁴https://gazebosim.org/docs/latest/ros2_integration/

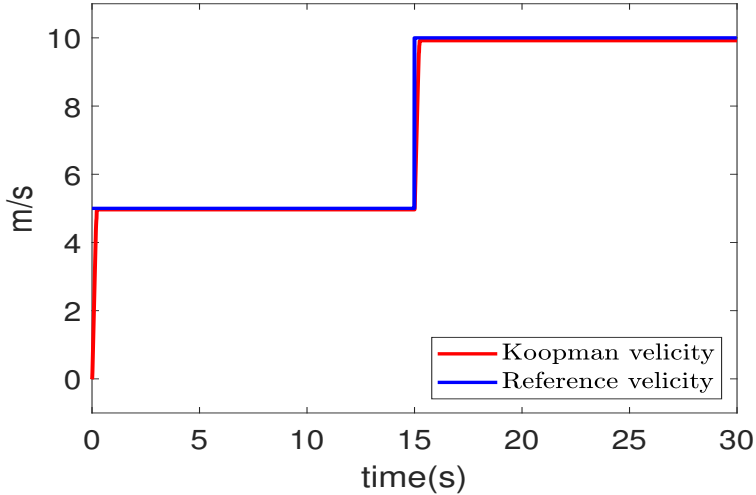


Figure 2: MPC control for the referring tracking

simulator incorporates Fossen’s equations (Fossen, 2011) to model hydrodynamics, similar to the approaches detailed in previous studies by Zhang et al. (2022a). This setup provides a more realistic test environment for AUV applications and algorithm design. Fig. 4 illustrates the experimental simulator, where the vehicle’s movement is powered by a stern thruster. There are four rudders: two vertical rudders control the AUV’s steering, while two horizontal rudders manage its ascent and descent. The speed of the AUV is controlled by adjusting the thruster’s velocity.

5.2.2. Simulation Process

Fistly, acquiring propeller speed and UAV’s velocity data. Using the `rosgz_bridge` package, the topics controlling the propeller and the 3D orientation of the underwater vehicle in Gazebo are linked with the publisher and subscriber topics in ROS. This integration allows us to obtain information

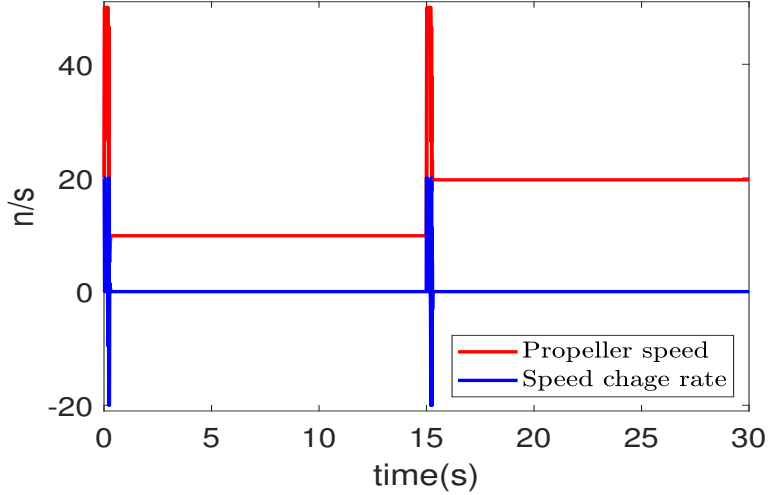
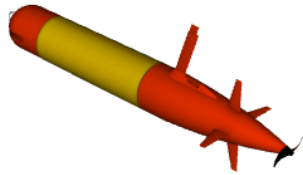
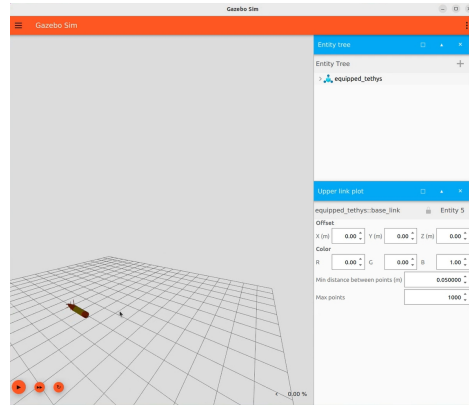


Figure 3: The input and input change rate signal

about the vehicle, including propeller speed and vehicle orientation, within the ROS system. The propeller speed, randomly generated within the range of $[-10, 10]$, is published by a ROS publisher. Concurrently, a subscriber records the vehicle's velocity. By running the simulation for a certain period, we obtain data on propeller speed and vehicle velocity. In this experiment, the data collection frequency is set to $10Hz$. Secondly, we use the collected data and the proposed algorithm to derive a high-dimensional linear matrix. This step is implemented in MATLAB 2022b. Finally, the computed matrices $\{A B C\}$ are loaded into ROS. Within a subscriber, the MPC algorithm is implemented using the `scipy.optimize` library. This algorithm calculates the propeller speed input based on the vehicle's velocity data from Gazebo. The calculated speed is then sent to Gazebo through a publisher which adjusts the vehicle velocity. The vehicle is tasked with tracking a piecewise continuous reference signal. For this experiment, we set $Q_s = Q_u = 2000$ and $R = 0.01$.



(a) The Laruv underwater vehicle



(b) The simulated platform

Figure 4: The simulated underwater vehicle and platform

The input propeller speed s is constrained within $[-150, 150]$, with the increment input restricted to $[-50, 50]$. A piecewise reference $y_r(t)$ is tracked. The lift function and simulation settings are identical to the simulation in MATLAB.

Fig. 5 shows the process of the experiment. Fig. 6 demonstrates the vehicle’s speed tracking using the proposed algorithm, with dynamic plots providing a more intuitive display of the process. As shown in the figure, the vehicle effectively follows the given reference signal even when the target speed changes, despite the constraints on propeller speed. This performance highlights the superiority of the MPC algorithm.

6. Conclusion

This paper introduces a control strategy for AUVs that integrates a data-driven Koopman MPC. The approach adeptly manages the multivariable nonlinear dynamics of AUVs, addressing state, input, and increment in-

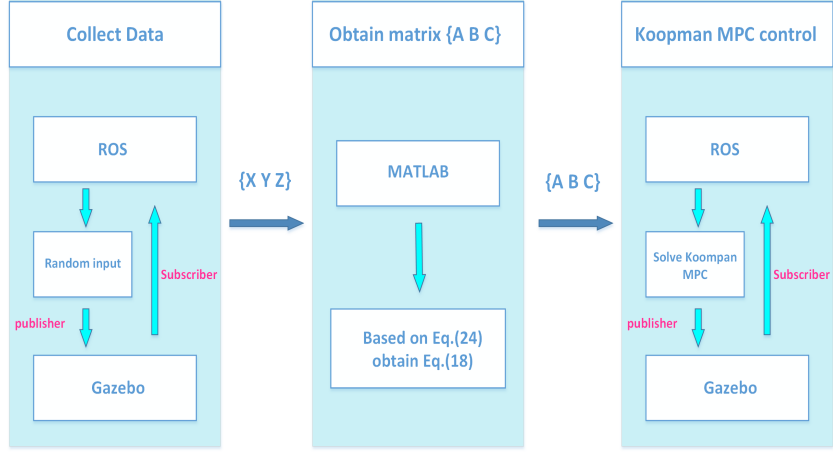


Figure 5: The experiment process

put constraints to ensure operational stability and performance. Validated through a ROS2 and Gazebo-based platform, our method shows effectiveness in complex underwater environments, offering a significant advancement for AUV control systems. The proposed strategies pave the way for more efficient and safer underwater exploration, with potential for further development and real-world application.

7. CRediT authorship contribution statement

Zhiliang Liu: Original draft, Methodology, Project administration, Formal analysis, Data curation, Conceptualization. **Xin Zhao:** Investigation, Review and editing. **Peng Cai:** Visualization, Validation, Methodology. **Bing Cong:** Validation, Review and editing.

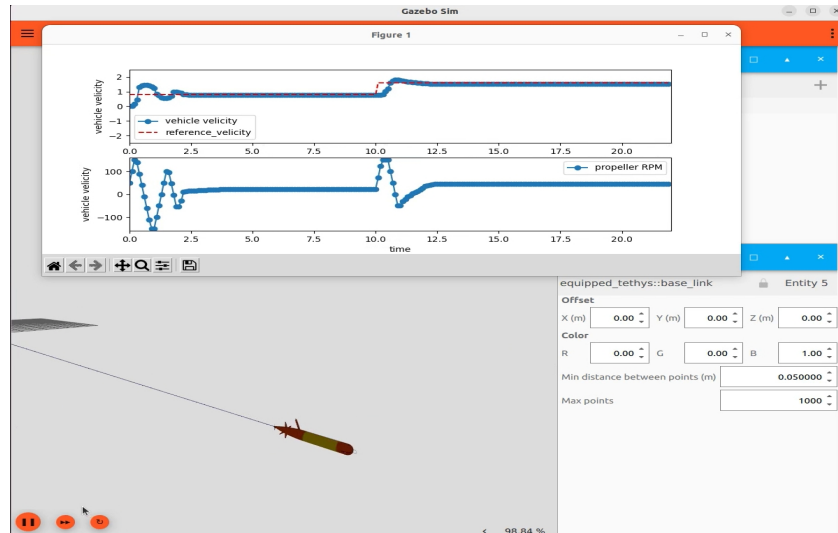


Figure 6: The experiment result

8. Declaration of competing interest

The authors declare that they have no known competing financial interests or personal relationships that could have appeared to influence the work reported in this paper.

9. Data availability

Data will be made available on request. The experiment video can be found at here.

10. Acknowledgment

This work was supported by Natural Science Foundation of China under grant 61873137.

References

- Bachmayer, R., Whitcomb, L.L., 2003. Adaptive parameter identification of an accurate nonlinear dynamical model for marine thrusters. *J. Dyn. Sys., Meas., Control* 125, 491–494.
- Bruder, D., Fu, X., Gillespie, R.B., Remy, C.D., Vasudevan, R., 2020. Data-driven control of soft robots using koopman operator theory. *IEEE Transactions on Robotics* 37, 948–961.
- Budišić, M., Mohr, R., Mezić, I., 2012. Applied koopmanism. *Chaos: An Interdisciplinary Journal of Nonlinear Science* 22.
- Di Vito, D., Antonelli, G., 2017. The effect of the ocean current in the thrusters closed-loop performance for underwater intervention, in: *OCEANS 2017-Anchorage*, IEEE. pp. 1–6.
- Fossen, T.I., 2011. *Handbook of marine craft hydrodynamics and motion control*. John Wiley & Sons.
- Gafurov, S.A., Klochkov, E.V., 2015. Autonomous unmanned underwater vehicles development tendencies. *Procedia Engineering* 106, 141–148.
- Gertler, M., Hagen, G.R., 1967. Standard equations of motion for submarine simulation. Technical Report. Naval Ship Research and Development Center.
- Gong, P., Yan, Z., Zhang, W., Tang, J., 2021. Lyapunov-based model predictive control trajectory tracking for an autonomous underwater vehicle with external disturbances. *Ocean Engineering* 232, 109010.

- Healey, A.J., Marco, D., 1992. Slow speed flight control of autonomous underwater vehicles: Experimental results with nps auv ii, in: ISOPE International Ocean and Polar Engineering Conference, Isope. pp. ISOPE–I.
- Healey, A.J., Rock, S., Cody, S., Miles, D., Brown, J., 1995. Toward an improved understanding of thruster dynamics for underwater vehicles. *IEEE Journal of oceanic Engineering* 20, 354–361.
- Kim, J., Chung, W.K., 2006. Accurate and practical thruster modeling for underwater vehicles. *Ocean Engineering* 33, 566–586.
- Koopman, B.O., 1931. Hamiltonian systems and transformation in hilbert space. *Proceedings of the National Academy of Sciences* 17, 315–318.
- Korda, M., Mezić, I., 2018. Linear predictors for nonlinear dynamical systems: Koopman operator meets model predictive control. *Automatica* 93, 149–160. doi:10.1016/j.automatica.2018.03.046.
- Kutz, J.N., Brunton, S.L., Brunton, B.W., Proctor, J.L., 2016. *Dynamic mode decomposition: data-driven modeling of complex systems*. SIAM.
- Lin, Y.H., Yu, C.M., Wu, I.C., Wu, C.Y., 2023. The depth-keeping performance of autonomous underwater vehicle advancing in waves integrating the diving control system with the adaptive fuzzy controller. *Ocean Engineering* 268, 113609.
- Mezić, I., 2005. Spectral properties of dynamical systems, model reduction and decompositions. *Nonlinear Dynamics* 41, 309–325.

- Player, T.R., Chakravarty, A., Zhang, M.M., Raanan, B.Y., Kieft, B., Zhang, Y., Hobson, B., 2023. From concept to field tests: Accelerated development of multi-auv missions using a high-fidelity faster-than-real-time simulator, in: 2023 IEEE International Conference on Robotics and Automation (ICRA), IEEE. pp. 3102–3108.
- Rowley, C.W., Mezić, I., Bagheri, S., Schlatter, P., Henningson, D.S., 2009. Spectral analysis of nonlinear flows. *Journal of fluid mechanics* 641, 115–127.
- Sahoo, A., Dwivedy, S.K., Robi, P., 2019. Advancements in the field of autonomous underwater vehicle. *Ocean Engineering* 181, 145–160.
- Schmid, P.J., 2010. Dynamic mode decomposition of numerical and experimental data. *Journal of fluid mechanics* 656, 5–28.
- Shen, C., Shi, Y., Buckham, B., 2017. Trajectory tracking control of an autonomous underwater vehicle using lyapunov-based model predictive control. *IEEE Transactions on Industrial Electronics* 65, 5796–5805.
- Williams, M.O., Kevrekidis, I.G., Rowley, C.W., 2015. A data-driven approximation of the koopman operator: Extending dynamic mode decomposition. *Journal of Nonlinear Science* 25, 1307–1346.
- Yan, Z., Wang, M., Xu, J., 2019. Robust adaptive sliding mode control of underactuated autonomous underwater vehicles with uncertain dynamics. *Ocean Engineering* 173, 802–809.
- Yan, Z., Yan, J., Cai, S., Yu, Y., Wu, Y., 2023. Robust mpc-based trajectory

- tracking of autonomous underwater vehicles with model uncertainty. *Ocean Engineering* 286, 115617.
- Yoerger, D.R., Cooke, J.G., Slotine, J.J., 1990. The influence of thruster dynamics on underwater vehicle behavior and their incorporation into control system design. *IEEE Journal of Oceanic Engineering* 15, 167–178.
- Zhang, B., Ji, D., Liu, S., Zhu, X., Xu, W., 2023. Autonomous underwater vehicle navigation: a review. *Ocean Engineering* 273, 113861.
- Zhang, M.M., Choi, W.S., Herman, J., Davis, D., Vogt, C., McCarrin, M., Vijay, Y., Dutia, D., Lew, W., Peters, S., et al., 2022a. Dave aquatic virtual environment: Toward a general underwater robotics simulator, in: 2022 IEEE/OES Autonomous Underwater Vehicles Symposium (AUV), IEEE. pp. 1–8.
- Zhang, X., Pan, W., Scattolini, R., Yu, S., Xu, X., 2022b. Robust tube-based model predictive control with koopman operators. *Automatica* 137, 110114.